August 27-31, 2023
FLORENCE - ITALY
ICWE 16
16th International Conference on Wind Engineering

# Large eddy simulation of vortex-induced forces on an oscillating circular cylinder in subcritical regime

Ruilin Zhang [1], Zhiwen Liu [1,2], Zhengqing Chen [1,2]

[1]*Key Laboratory for Wind & Bridge Engineering of Hunan province, Hunan University, Changsha, China*
[2]*College of Civil Engineering, Hunan University, Changsha, China*

**SUMMARY:**
In this study, vortex-induced force characteristics of a circular cylinder at a higher subcritical Reynolds number are investigated by using three-dimensional large eddy simulations of forced oscillation. The simulations of the oscillating cylinder are performed under a series of amplitudes and at a fixed reduced velocity. The numerical results are presented in terms of integral forces, spanwise correlations and pressure distributions. It is shown that the oscillation amplitude has obvious effects on the magnitude and phase of motion-induced lifts. Meanwhile, the correlation of overall forces is relatively weak, while the motion-induced forces are almost fully correlated except in the phase jump regime. Also, two modes of pressure distribution are observed with regard to small- and large-amplitude states.

*Keywords: circular cylinder, unsteady aerodynamic forces, large eddy simulation.*

## 1. GENERAL INSTRUCTIONS

Vortex-induced vibration (VIV) for circular cylinder cases is of practical significance in many engineering fields, i.e., bridge cables, chimney stacks, and marine risers. In this sense, the vortex-induced forces (VIF) are always a concerning issue, which is the key to understanding, predicting and even preventing VIV behaviour.

VIFs can be measured through free- or forced-oscillation tests. However, it is relatively difficult to measure the oscillation and force simultaneously through experimental technology. On the other hand, the computational fluid dynamics (CFD) method has distinct advantages of studying the force characteristics in detail. Considering the computational costs, however, most of the numerical studies are performed by using two-dimensional Reynolds-Averaged Navier-Stokes (RANS) simulations (Pan et al., 2007) or focusing on the low Reynolds number flow of $Re$=10-$10^3$ (Zhao et al., 2014). Recently, large eddy simulation (LES) is attempted to predict the cylinder VIV in the higher-$Re$ subcritical regime (Pastrana et al., 2018). Nevertheless, the LES study of oscillating cylinders in the higher Reynolds number regime (i.e., $Re > 10^4$) is still limited up to now.

In this study, vortex-induced forces of a circular cylinder in the higher-$Re$ subcritical regime are comprehensively investigated by means of 3D LES and the forced-oscillation method.

## 2. NUMERICAL MODEL

The three-dimensional transient flow can be determined by the unsteady Navier-Stokes (N-S) equations together with the LES model, where the variables are spatially filtered according to the grid scale. For incompressible flow, the filtered N-S equations in the arbitrary Lagrangian-Eulerian (ALE) scheme can be written as:

$$\frac{\partial \tilde{u}_i}{\partial x_i} = 0,\ \frac{\partial \tilde{u}_i}{\partial t} + \frac{\partial \tilde{u}_i}{\partial x_j}\left(\tilde{u}_j - \hat{u}_j\right) = -\frac{1}{\rho}\frac{\partial \tilde{p}}{\partial x_i} + \nu\frac{\partial^2 \tilde{u}_i}{\partial x_j^2} - \frac{\partial \tau_{ij}}{\partial x_j} \tag{1}$$

where $\rho$ is air density; $t$ is the time; $x_i$ is the Cartesian coordinate; $u_i$ is the filtered velocity component, and $u_j$ is the velocity component of mesh moving; $p$ is the filtered pressure. Moreover, the wall-adapting local-eddy viscosity model (WALE) is herein employed to calculate the sub-grid eddy viscosity. The governing equations for airflow are solved in a three-dimensional computational domain, which is spatially discretized by using structured grids. After convergence studies, the total grid number of the model is 1.78 million, as shown in Fig. 1. Moreover, the numerical model is validated by performing the simulation of flow over a stationary cylinder.

The unsteady aerodynamic forces on the cylinder are herein determined by employing the forced-oscillation method, where the rigid cylinder is controlled by a prescribed harmonic motion as: $y(t) = A_y^* sin\omega t$, where $A_y^*$ and $\omega = 2\pi f$ are the normalized oscillation amplitude and frequency, respectively.

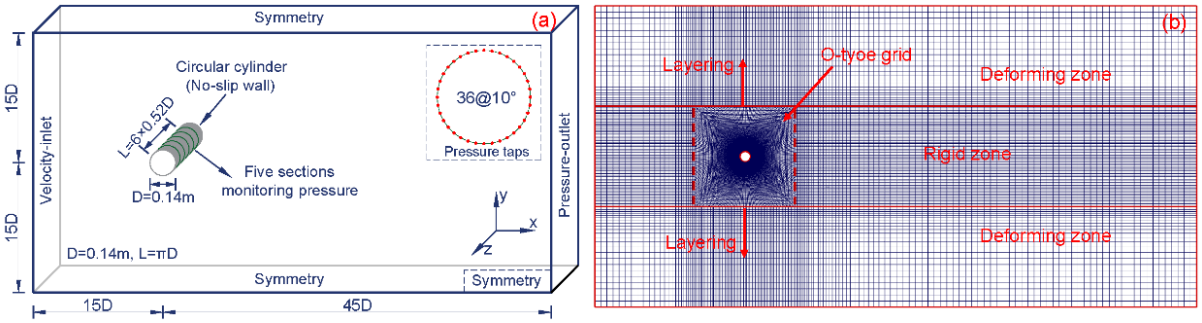


**Figure 1.** CFD model of the circular cylinder: (a) computational domain; (b) grid resolution in x-y plane.

## 3. RESULTS AND DISCUSSION

The forced oscillation of the circular cylinder is simulated under a series of normalized amplitudes ranging from 0.05 to 0.60 with a step of 0.05. Whereas, this study focuses on only one reduced velocity of 6.0, around which the peak amplitude of VIV usually occurs (Feng, 1968). The Reynold number is fixed at $Re = 2.01 \times 10^4$.

### 3.1. Integral aerodynamic forces

We illustrate the energy properties of the aerodynamic force through the lift coefficient-displacement diagram ($C_L - y$) of the oscillating cylinder, as shown in Fig. 2. Furthermore, the motion-induced forces are separated from overall forces by using inverse Fourier transform, as shown with red lines in Fig. 2. Obviously, for the motion-induced force, the phase diagrams are ellipses in shape and rotate in clockwise directions as the time increases for all cases, which

indicates that the lift has positive energy contribution in one period. However, the shapes of phase diagrams are quite varied with the vibration amplitudes. Specifically, the diagrams are squeezed horizontally as $A_y^*$ increases from 0.05 to 0.20, and then become generally narrower when $A_y^*$ is larger than 0.25. As a result, the diagram area decreases as $A_y^*$ increases, indicating the decrease of the energy-trapping capability from flow because the figure scale is proportional to the oscillation amplitude. The flattening and narrowing of the diagram are associated with the variation of relative magnitude and phase of motion-induced force, respectively.

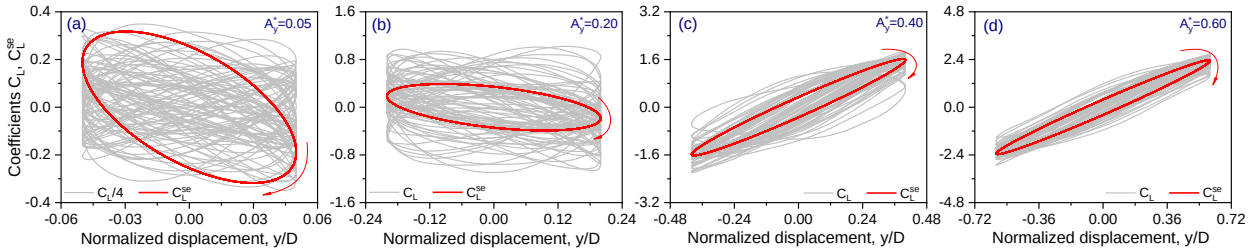


**Figure 2.** Phase diagram of lift coefficients and displacements of the oscillating cylinder under various amplitudes: (a) $A_y^* = 0.05$; (b) $A_y^* = 0.20$; (c) $A_y^* = 0.40$; (d) $A_y^* = 0.60$.

### 3.2. Spanwise correlation

The variation of sectional lift forces along the cylinder span can be quantified by the correlation coefficient between two locations at $z_1$ and $z_2$, which is defined by $R = \overline{C_L(z_1)C_L(z_1)}/[\sigma_{C_L(z_1)}\sigma_{C_L(z_2)}]$, where the over-bar represents averaging. The calculated correlation coefficients of sectional lift forces under different vibration amplitudes are shown in Fig. 3. Moreover, the stationary cylinders' results from the present simulation and previous experiment (Blackburn, 1994) are also drawn in Fig. 3 for comparison. It is seen that the correlation coefficients of the overall lift forces decrease as the spanwise distance increases, but the decaying rates depend highly on the oscillation amplitude. For the minor oscillation amplitude of $A_y^*$=0.05, the correlation is close to but slightly higher than that of the stationary cylinder. As the oscillation amplitude increases, the correlation coefficient decreases firstly and reaches a minimum value at $A_y^* = 0.20$, then increases gradually up to $R(2.1D) = 0.81$ at $A_y^* = 0.60$. On the other hand, the motion-induced lift forces have almost full correlations in the studied spanwise length, except for $A_y^* = 0.20$.

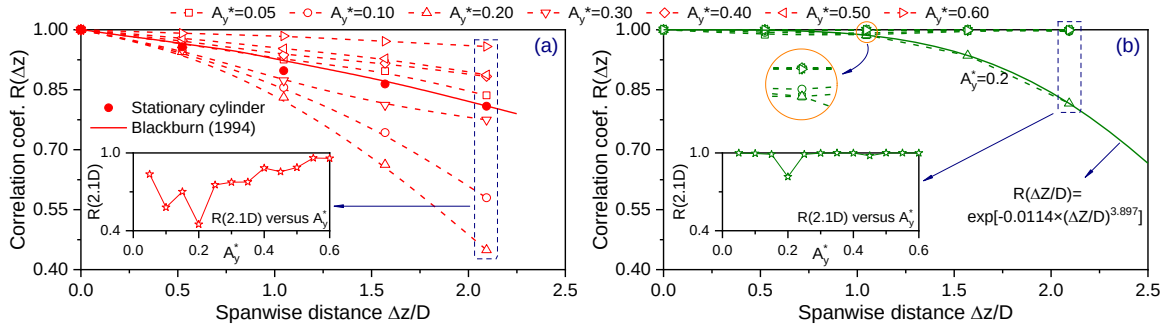


**Figure 3.** Correlation coefficients of sectional lift forces on the oscillating cylinder along the spanwise distance: (a) overall lift forces; (b) motion-induced lift forces.

### 3.3. Pressure distribution

Fig. 4 shows the instantaneous and mean pressure coefficients around the cylinder during a cycle at four different instants. Referring to Fig. 4a, for the cylinder at small-amplitude state, the variation of the instantaneous pressure is relatively small and occurs only on the upper and lower surfaces of the cylinder. Referring to Fig. 4b, for the cylinder at large-amplitude state, the instantaneous pressure varies dramatically along with the change of motion vector. The two modes of pressure distribution imply different aerodynamic mechanisms.

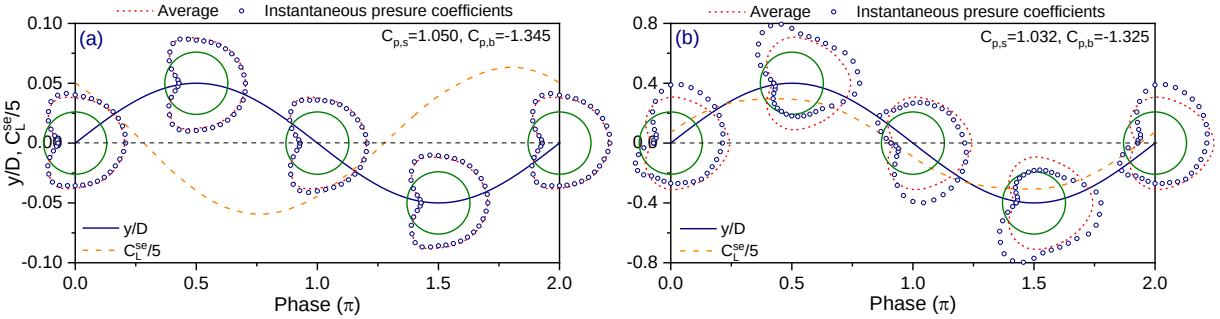


**Figure 4.** Instantaneous pressure distribution around the oscillating cylinder under various oscillation amplitude: (a) $A_y^* = 0.05$; (b) $A_y^* = 0.40$.

## 4. CONCLUSIONS

This study addresses the vortex-induced force characteristics of an oscillating circular cylinder in the subcritical regime ($Re$=2.0×10$^4$) by means of large eddy simulation. Some conclusions can be drawn as follows: (i) The oscillation amplitude has obvious effects on the motion-induced lifts involving both magnitude and phase. (ii) The spanwise correlation of overall forces decreases firstly and then increases as the oscillation amplitude increases. Whereas, the motion-induced forces are almost fully correlated along the cylinder span except in the transient regime. (iii) Two modes of pressure distribution are observed with regard to small- and large-amplitude states.


#### ACKNOWLEDGEMENTS

This research was financially supported by the National Natural Science Foundation of China (Grant No. 52178475, 51778225), for which the authors are grateful.


#### REFERENCES


Blackburn, H.M., 1994. Effect of blockage on spanwise correlation in a circular cylinder wake. Experiments in Fluids. 18, 134-136.

Feng, C.C., 1968. The measurement of vortex induced effects in flow past stationary and oscillating circular and D-section cylinders. Master's thesis, University of British Columbia.

Pastrana, D., Cajas, J.C., Lehmkuhl, O., Rodr ́guez, I., Houzeaux, G., 2018. Large-eddy simulations of the vortex-induced vibration of a low mass ratio two-degree-of-freedom circular cylinder at subcritical Reynolds numbers. Computers and Fluids. 173, 118-132.

Pan, Z.Y., Cui, W.C., Miao, Q.M., 2007. Numerical simulation of vortex-induced vibration of a circular cylinder at low mass-damping using RANS code. Journal of Fluids and Structures. 23, 23-37.

Zhao, M., Cheng, L., An, H., Lu, L., 2014. Three-dimensional numerical simulation of vortex-induced vibration of an elastically mounted rigid circular cylinder in steady current. Journal of Fluids and Structures. 50, 292-311.